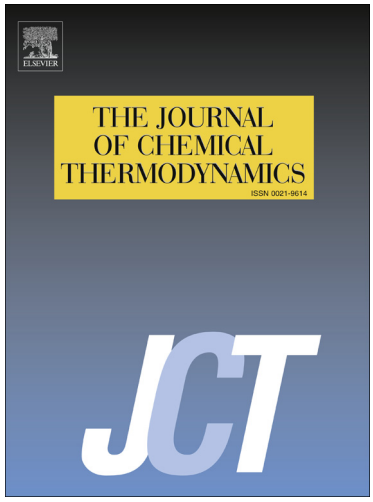

Thermodynamic analysis of unimer-micelle and sphere-to-rod micellar transitions of aqueous solutions of sodium dodecylbenzenesulfonate

Artur J.M. Valente, José J. López Cascales, Antonio J. Fernández Romero

PII: S0021-9614(14)00148-7
DOI: http://dx.doi.org/10.1016/j.jct.2014.05.001
Reference: YJCHT 3928

To appear in: *J. Chem. Thermodynamics*

Received Date: 20 December 2013
Revised Date: 25 April 2014
Accepted Date: 1 May 2014

Please cite this article as: A.J.M. Valente, J.J. López Cascales, A.J. Fernández Romero, Thermodynamic analysis of unimer-micelle and sphere-to-rod micellar transitions of aqueous solutions of sodium dodecylbenzenesulfonate, *J. Chem. Thermodynamics* (2014), doi: http://dx.doi.org/10.1016/j.jct.2014.05.001

Thermodynamic analysis of unimer-micelle and sphere-to-rod micellar transitions of aqueous solutions of sodium dodecylbenzenesulfonate

Artur J. M. Valente[1]

[1]*Department of Chemistry, University of Coimbra, 3004-535 Coimbra, Portugal*

José J. López Cascales[2] and Antonio J. Fernández Romero[3*]

[2]*Grupo de Bioinformática y Macromoléculas (BIOMAC), Universidad Politécnica de Cartagena, Aulario II, Campus de Alfonso XIII, Cartagena, Murcia 30203, Spain*

[3] *Grupo de Materiales Avanzados para la Producción y Almacenamiento de Energía, Universidad Politécnica de Cartagena, Aulario II, Campus de Alfonso XIII, Cartagena, Murcia 30203, Spain*

Abstract

Temperature dependence of specific conductivity of sodium dodecylbenzenesulfonate (NaDBS) aqueous solutions was analyzed. Two breaks on the plot appeared for all temperature, which suggest two micellar transitions. This has been corroborated by surface tension measurements. The first transition concentration occurs at the critical micelle concentration (CMC), whilst the second critical concentration (so-called transition micellar concentration, TMC) is due to a sphere-to-rod micelles transition. The dependence of CMC and TMC on the temperature allows the computation of the corresponding thermodynamic functions: Gibbs free energy, enthalpy and entropy changes. For the CMC, enthalpy and entropy increments were found that decrease with the temperature values. However, an anomalous behaviour was obtained for the TMC, where both ΔS^0 and ΔH^0 values raised with the temperature

[*]Corresponding author (A.J.F.R.): antonioj.fernandez@upct.es
Phone: +34 968325580. Fax. +34. 968 325931.

increase. However, for both transitions, an enthalpy-entropy compensation is observed. These results will be compared with similar systems reported in the literature.

Keywords: sodium dodecylbenzenesulfonate; electrical conductivity; critical micelle concentration; transition micellar concentration; sphere-to-rod transition; micellization thermodynamics;

1. Introduction

It is well known that amphiphilic molecules form aggregates in aqueous solution when concentration is higher than its critical micelle concentration (CMC). Many experimental magnitudes can be studied to detect the CMC in aqueous solution, such as conductivity, viscosity, refractive index or surface tension [1-3].

Moreover, it has been frequently reported that a second change of the physicochemical properties of the surfactant solutions appears at concentrations above the first CMC. This second change has been determined for numerous surfactants by different experimental methods and it has been termed as the second CMC or second transition micellar concentration (TMC hereafter) [4-10]. Conductivity measurements have been considered one of the most straightforward methods to obtain information about the second CMC, due to its high sensitivity and reproducibility [4]. Several authors have interpreted this second CMC as due to structural micellar changes, most likely a sphere to rod-like transition.

Formation of different micelle shapes aggregates has been previously proposed for sodium dodecylbenzenesulfonate (NaDBS), or other alkyl-benzenesulfonates solutions: also spherical micelles, ellipsoid, rodlike, wormlike, and bilayer structures [11-15] Molecular Dynamic [11] and NMR studies [12] have shown evidence of NaDBS micelle shape transformations from spherical to more complex micellar aggregates. Also, species accompanying NaDBS can dramatically affect the structural micellar transition from spherical to rod-like or other micellar structures [16,17].

Recently we used electrical conductivity, viscosimetry and cyclic voltammetric measurements to demonstrate a second micellar transition occurring in NaDBS aqueous medium, at concentrations around 0.1 M. [15] Furthermore, we observed how the structural micellar transition of the NaDBS surfactant influences the potentiodynamic polymerization and the final morphology of polypyrrole/DBS synthesized using monomer-NaDBS aqueous solutions.

Temperature dependence of CMC for aqueous solutions of ionic and nonionic surfactants has been frequently reported, usually obtaining a concave-shaped with a minimum at a characteristic temperature, labeled as T^*. Hence, Gibbs free energy, enthalpy and entropy changes of micellization, as a function of temperature, have been estimated [5,10,20,21].

However, there are few papers where a thermodynamic analysis of the second transition concentration (TMC) of surfactants with temperature was carried out.

Gonzalez et al. have reported different surfactants exhibiting two micellar transitions. They showed that CMC values versus temperature form a concave curve, while TMC values show a convex curve [8-10]. However, no thermodynamic analysis involving the computation of ΔS^0 and ΔH^0, as a function of temperature, for both micellar transitions has been reported, to the best of our knowledge.

The aim of this paper is to investigate how the CMC and TMC values of NaDBS change with the temperature and, from here, to analyze how thermodynamic parameters are modified with temperature change. We present for the first time a comprehensive thermodynamic analysis, including the Gibbs free energy, enthalpy and entropy changes, for the two micellar transitions for aqueous solutions of sodium dodecylbenzenesulfonate. This thermodynamic analysis demonstrates that ΔS^0 and ΔH^0 values diminish with temperature for the CMC, while ΔS^0 and ΔH^0 increase with the temperature for the TMC. This opposite behavior has been corroborated by the results obtained for dodecyldimethylbenzylammonium bromide (C_{12}BBr) surfactant, which exhibited two micellar transitions too, when ΔS^0 and ΔH^0 were calculated by us from the CMC and TMC values previously reported [8]. Moreover, thermodynamic parameters of the two surfactants were calculated using the charged pseudo-phase separation model of micellization and the Muller's treatment for both micellar transitions resulting in good agreement.

We have also found for the TMC of NaDBS and C_{12}BBr surfactants a linear relationship between enthalpic and the entropic contributions, as it was reported frequently for the CMC of different surfactants [18, 19, 22-25]. All of thermodynamic results obtained are discussed for a better understanding of the ΔS^0 and ΔH^0 variation with the temperature and the stability differences between spherical and non-spherical micelles.

2. Experimental

2.1 Reagents

Sodium dodecylbenzenesulfonate (Aldrich, with 0.98 mass fraction purity) was used as received. This compound is a mixture of different isomers, prevailing the p-dodecylbenzenesulfonate. A total of 26 different concentrations of NaDBS solutions were prepared ranging between (1.05×10^{-4} and 2.35×10^{-1}) mol Kg^{-1}. Solutions were freshly prepared previous to the measurements. To obtain a good solution free of bubbles a JP Selecta Ultrasonic was used. Millipore water with resistivity of > 18 MΩ cm was used.

2.2 Apparatus and procedure

Direct Current (DC) Conductivities have been measured with a Crison M-Basic 30 Conductivity Meter. A dip type cell with platinum electrodes was used and calibrated with a standard solution (12.88 or 1.413) mS cm^{-1} at T=298.15 K and P=1.01×10^{5} Pa.

The solutions were prepared by weight using an analytical balance with an uncertainty of ±0.1 mg and the molalities calculated found to be uncertain to ±0.0002 mol kg^{-1}. The specific conductance of the solution was measured after each addition and corresponds to the average of three independent measurements. Specific conductance values and their standard deviation are listed in SM1 and SM2 tables, in supplementary material. Temperature control was carried out with a Julabo EH F-25 thermostat. Temperature was changed between (283.15 and 313.15) K, in steps of 5 K. The temperature has been controlled within ±0.02 K. Previous to carrying out each measure we wait 15 minutes to obtain a stable value.

Surface tension values of NaDBS aqueous solutions, in the concentration range 2.6 $x10^{-4}$ to 0.19 mol kg^{-1}, were measured by the du Nouy ring method based on force measurements, using a Lauda-Brinkman tensiometer TD 3. The uncertainty of the surface tension measurements is (±0.04) $mN.m^{-1}$. The measurements were carried out over the temperature range from (298.15 to 313.15) K and atmospheric pressure. The sample under measurement was kept thermostated in a double-jacketed glass cell by means of Thermo Scientific Phoenix II B5 thermostat bath, equipped with a Pt100 probe. The temperature has been controlled within ±0.02 K. All solutions were prepared

in Millipore-Q water. Surface tension data shown in Figure 3 are average values of, at least, 5 independent measurements. Experimental surface tensions of water, γ_0, at different temperatures are: γ_0=72.0 (±0.1) mN.m^{-1} (T=298.15 K), γ_0=71.1 (±0.2) mN.m^{-1} (T=303.15 K), γ_0=70.3 (±0.2) mN.m^{-1} (T=308.15 K) and γ_0=69.4 (±0.2) mN.m^{-1} (T=313.15 K), respectively. These values are in close agreement with those reported by Vargaftik et al. [26]. Experimental relative surface tension values and their standard deviation are listed in table SM3, in supplementary material.

3. Results

The NaDBS specific electrical conductance shows three different linear regimes as a function of surfactant concentration, for seven different temperatures, ranging between 283 and 313 K (Figure 1). The first slope change occurring at lower NaDBS concentrations are attributed to the critical micelle concentration (CMC). At 298.15 K the CMC appears at 4.2×10^{-3} mol Kg^{-1}.

A second slope change appears at *ca.* 0.1 M, which may be assigned to a second micelle transition (TMC), where a structural transition of the micellar aggregates occurs, probably from spherical to rod-like or more complexes micellar aggregates, such as it has been previously reported for this surfactant [11-15].

Figure 1

CMC and TMC values were calculated by using the interception of the data regression lines method at pre- and post-break regions. The fitting of a straightline equation to experimental data, at different concentrations range, led to regression coefficients higher than 0.998. Figure 2 shows the dependence of CMC and TMC molar fractions on the temperature. As can be seen, variation of CMC values with temperature shows a concave-shape curve, as it has been observed frequently for different surfactants [8,9,18,28]. However, temperature dependence of TMC values shows a convex-shaped curve. A similar behavior has been reported for the second breaks observed for different surfactants [8, 9].

Figure 2

The slope changes observed in conductivity measurements (Figure 1) are explained by the variation of degree of counterion dissociation of micelles, β [5, 29]. β values can be calculated from the ratio between the slope above each break points (S_2 and S_3) and the slope at pre-micelle region (S_1), in the plots of $\sigma=f$([NaDBS]). Consequently, for the CMC, $\beta = S_2/S_1$ [30] and for the TMC, $\beta_t = S_3/S_1$ (see, for example, ref. [5, 29, 32]) where S_2 and S_3 are slopes for the concentration range between CMC and TMC and above TMC, respectively (see Figure 1). It should be highlighted that the

calculation of β and β_t is done on the basis of an existence of an equilibrium between surfactant unimers and micelles, either in spherical or cylindrical shape, respectively.

Figure 3

The dependence of β and β_t values on temperature is displayed in Figure 3, where β values are higher than β_t values for all temperature range, as it was reported previously. [4,5,8] A light increase with temperature was obtained for β value, while β_t was quasi constant at temperature below 300 K and after that, it increased quickly.

In order to verify the dependence of the CMC on the temperature as well as the second transition point observed by electrical conductance measurements, surface tension measurements were carried. Figure 4 shows the effect of temperature and NaDBS aqueous solution concentration on the surface tension. It is clear seen that the surface tension (γ) decreases initially with increasing concentration and then a distinct break point appears indicating the formation of micelles. It is worth mentioning that the absence of a minimum around that breakpoint indicated that no impurities are affecting the measure [33]. Upon increasing of NaDBS concentration a second breakpoint is observed, which can be related with sphere-to-rod transition, as deeply discussed by Alargova et al. [34] Following the previous discussion both transitions points corresponds to the CMC and TMC and are shown in Table 1. It should also be stressed that by increasing the temperature the surface tension behavior at the post-micelle region shows a slight decrease with concentration, which can be related with a closely packed surfactant adsorption at air-aqueous solution interface [35].

Figure 4

CMC values obtained by surface tension are lower than those obtained by electrical conductivity. It should be stressed that electrical conductivity and surface tension measurements are sensitive to different physical properties and consequently it is not unusual to obtain different critical values for the same system [33].. Whatever, all of the CMC values are in agreement with the values range reported previously, from 6.4×10^{-4} to 4×10^{-3} mol L^{-1} [1,6,15,27,36]. Also, we can observe that the variation of CMC and

TMC with the temperature have the same tendency for the values obtained by surface tension and conductivity measurements.

Table 1

3.1 Thermodynamics of micellization

In accordance with the charged pseudo-phase separation model of micellization for ionic surfactant [7, 18], we may estimate the Gibbs free energies of micellization at the CMC and TMC, by

$$\Delta G_m^o = (2-\beta)RT \ln \chi_{cmc} \quad (1)$$

$$\Delta G_t^o = (2-\beta_t)RT \ln \chi_{tmc} \quad (2)$$

where R is the gas constant, T is the temperature and χ_{cmc} and χ_{tmc} are the molar fractions at the CMC and TMC obtained by conductivity measurements. Figure 5 shows the ΔG^0_m and ΔG^0_t values versus temperature. As can be seen, all free energies measured are negative and their values decrease with temperature. Furthermore, ΔG^0_m values are more negative than ΔG^0_t for all the considered temperature range.

Figure 5

The ΔG^0_m and ΔG^0_t values have been used to obtain the standard enthalpy of aggregation, ΔH^0_m and ΔH^0_t, by applying the Gibbs-Helmholtz equation:

$$\Delta H_m^o = -RT^2(2-\beta)\left[d \ln \chi_{cmc}/dT\right] \quad (3)$$

$$\Delta H_t^o = -RT^2(2-\beta_t)\left[d \ln \chi_{tmc}/dT\right] \quad (4)$$

To evaluate the enthalpies, $(d\ln\chi_{cmc}/dT)$ and $(d\ln\chi_{tmc}/dT)$ were calculated by fitting the $\ln\chi_{cmc}$, and $\ln\chi_{tmc}$, versus T data to a second order polynomial and differentiation.

Figure 6.A shows ΔH^0_m and ΔH^0_t versus temperature for NaDBS surfactant. ΔH^0_m decreases with temperature increment, in agreement with that usually reported previously [18,19,22,23]. In this case, it is observed that ΔH^0_m has endothermic values at lower temperature, and it decreases with the temperature, at T=298 K ΔH^0_m=0, coinciding with CMC minimum (see Figure 2). ΔH^0_m adopts negative values in higher temperature.

Figure 6

However, ΔH^0_t values increase with temperature values. At lower T, ΔH^0_t has negative values and it increases with the temperature, $\Delta H^0_t = 0$ at T=300 K, near the maximum observed in Figure 2. At higher temperatures endothermic values of ΔH^0_t are obtained.

The entropies of micellizations, ΔS^0_m and ΔS^0_t, were determined by the equations:

$$\Delta S_m^o = (\Delta H_m^o - \Delta G_m^o)/T \quad (5)$$

$$\Delta S_t^o = (\Delta H_t^o - \Delta G_t^o)/T \quad (6)$$

Both ΔS^0_m and ΔS^0_t values are positive in the whole temperature range studied (Figure 7.A). The results obtained for ΔS^0_m are in agreement with those reported previously for different surfactants: its value decreases with the temperature [23-26,28]. However, ΔS^0_t raising is observed with the temperature.

Figure 7

The anomalous temperature dependence obtained for ΔH^0_t and ΔS^0_t need to be examined in depth. With the aim of corroborating the increase in ΔH^0_t and ΔS^0_t with temperature we have calculated enthalpy and entropy values for the CMC and TMC of the surfactant dodecyldimethylbenzylammonium bromide (C_{12}BBr). This surfactant displays a CMC and TMC temperature dependence similar to NaDBS, this is, CMC values versus temperature produce a concave-shape curve, while the temperature dependence of CMT values shows a convex-shaped curve [8]. Figures 6.B and 7.B show the ΔH^0_m and ΔS^0_m, ΔH^0_t and ΔS^0_t values obtained using the CMC, TMC, β and β_t values reported in reference [8] and applying equations 3-6, as it has been explained above.

As can be seen, a similar tendency for ΔH^0_t and ΔS^0_t was obtained for this surfactant: both of them increase with temperature.

With the aim of confirming the thermodynamic quantities obtained from equations 3-6, and the enthalpies and entropies changes to the first and the second CMC, we used the Muller's treatment [37,38], which provides the next relation for the first CMC:

$$\ln \chi_{cmc} / \chi^{*}_{cmc} = \left[\Delta C^{o}_{p,m}(1 - T^{*}/T + \ln T^{*}/T)\right]/(2-\beta)R \quad (7)$$

where χ^{*}_{cmc} is the minimum χ_{cmc} value at temperature T^{*} and $\Delta C^{0}_{p,m}$ is the heat capacity change. We have also adapted this equation for the second micellar transition:

$$\ln \chi_{cmc} / \chi^{*}_{tmc} = \left[\Delta C^{o}_{p,t}(1 - T_t^{*}/T + \ln T_t^{*}/T)\right]/(2-\beta_t)R \quad (8)$$

where χ^{*}_{cmt} is the maximum χ_{cmt} value at temperature T_t^{*} and $\Delta C^{o}_{p,t}$ is the heat capacity change for the CMT.

Figure 8 displays the change of ln ($\chi_{cmc}/\chi^{*}_{cmc}$) vs. $(1-T^{*}/T+\ln T^{*}/T)\cdot 1/(2-\beta)R$ for the first CMC and ln ($\chi_{tmc}/\chi^{*}_{tmc}$) vs. $(1-T_t^{*}/T+\ln T_t^{*}/T)\cdot 1/(2-\beta_t)R$ for the TMC. This plot provides heat capacity values from the slopes, resulting $\Delta C^{0}_{p,m}$= -547.39 $J\cdot K^{-1}\cdot mol^{-1}$ and $\Delta C^{0}_{p,t}$= 554.29 $J\cdot K^{-1}\cdot mol^{-1}$.The heat capacity for the micelle formation shows a negative value similar to those reported for the micellization of ionic surfactants [39]Such a negative value can be explained by the removal of hydrocarbon chains from water. However, the heat capacity change for the TMC is similar in absolute value but positive. Such algebraic value has been reported by Islam and Kato [38]; they justified such a value as probably due to the crowding of a substantial number of water molecules around the headgroups of the surfactant, which outweighs the effect of the breakdown of the water structure upon micellization within the studied temperature range.

Figure 8

According to Muller's theory, the values of the enthalpy and entropy changes of micellization can be calculated by:

$$\Delta H^{o}_{m} = \Delta C^{o}_{p,m}(T - T^{*}) \quad (9)$$

$$\Delta S^{o}_{m} = \Delta S^{o*}_{m} + \Delta C^{o}_{p,m}\ln(T/T^{*}) \quad (10)$$

where

$$\Delta S_m^{o*} = -\Delta G_m^{o*} / T^* = -R(2-\beta)\ln(\chi_{cmc}) \quad (11)$$

We have observed that this treatment can be applied for the second transition.

$$\Delta H_t^o = \Delta C_{p,t}^o (T - T_t^*) \quad (12)$$

$$\Delta S_t^o = \Delta S_t^{o*} + \Delta C_{p,t}^o \ln(T/T_t^*) \quad (13)$$

where

$$\Delta S_t^{o*} = -\Delta G_t^{o*} / T_t^* = -R(2-\beta_t)\ln(\chi_{tmc}) \quad (14)$$

Enthalpy and entropy values obtained with the Muller's treatment are shown in figures 6.A and 7.A. As can be seen, the results are in good agreement with those obtained previously using equations 3-6 for the two micellar transitions.

4. Discussion

The occurrence of the first micellar point can be interpreted as due to a compensation effect of two different processes: the destruction of the orderly arrangement of water molecules around the hydrophobic chains of the surfactant (frequently named iceberg) when the micelles are formed; and the ordering of the randomly oriented amphiphile molecules from the solvated form into a micelle structure [18,19,22,23]. When temperature increases, the size of the iceberg around chains decreases due to melting, and thus less energy is required to break up the water structure. Hence, ΔH^0 values become more exothermic with the increment of temperature. With respect to ΔS^0, these two effects can be considered again, the first one is due to dehydration of water molecules from hydrocarbon chains, ΔS^0_w, which will be positive because it contributes to a major disorder. The second part, ΔS^0_{agg}, is related to the aggregated formation and its value will be negative, because the surfactant molecules are more ordered than in the solvent bulk. As the temperature increases the hydrogen bonds diminishes and ΔS^0_w values will decrease. This fact causes that ΔS decreases with temperature, as it can be observed in Figure 7.

Although this explanation is usually accepted, in the process of formation of spherical micelles other parameters may have a non-neglected contribution.These parameters are the degree of dissociation of counterions in micelles, solvation of the hydrophilic part of the surfactant molecules, counterions solvation, coulombic repulsion

of the hydrophilic heads, etc. In this sense, it has to be noted that a convex-shaped temperature dependence has also been observed for the CMC of ionic surfactants [38], which cannot be explained only by considering the dehydration of hydrocarbons chains and the interactions of the chains inside micelle aggregates.

Hence, the anomalous thermodynamic behavior found by us for the TMC needs a further explanation. The dependence of TMC on temperature for sodium octanoate [9] shows a convex-shaped profile, similar to that described in the present work (Figure 2). To explain this behavior, those authors consider two effects with the temperature rising: a) an increase in the dehydration of the headgroups and b) an increase in the thermal solubility of the surfactant monomers. Furthermore, the rising in the TMC values, below T_{max}, is a consequence of the dominating effect of thermal solubility of the molecules over dehydration of headgroups. Above T_{max}, TMC values decrease because dehydration of hydrophilic groups outweighs the thermal solubility of the molecules.

Continuing with this argument, we can use these two factors to explain why ΔS^0_t and ΔH^0_t grow with temperature. Regarding the rise of ΔS^0_t with the temperature, an increase of dehydration of headgroups favors a rising of the headgroups repulsions when the rod-like micelle is formed. Thus, increasing the temperature value will produce a higher repulsion between the hedagroups inside the micelle, it will raise the disorder and an increase in the ΔS^0_t values will be expected. With respect to the dependence of ΔH^0_t on temperature, when repulsion between headgroups rises, a higher energy would be required to form the micelle, making the process more endothermic. Furthermore, an increase in the thermal solubility of the surfactant monomers produces a stabilization of the monomers in the solution bulk, and a higher energy will be paid to form the micelles, resulting in more positive ΔH^0 values again.

Moreover, different data reported in the literature may help us to understand the ΔS^0_t and ΔH^0_t increase with temperature. Alauddin et al. [40] stated that spherical NaDBS micelles have to be more compact than rod-shaped micelles, even at higher temperatures. Hence, the hydrocarbon chains in the rod-like micelles will present a major flexibility than spherical ones, where the hydrocarbon chains will be probably more restricted. From this, the orientations and bendings of hydrocarbon chains will be more disordered in rod-like micelles, increasing ΔS^0_t values. Furthermore, this effect would be enhanced with temperature increase.

It is known that the micellar aggregation number decreases with the increase in temperature and the smaller aggregates are entropically favored over larger ones

[41,42]. Thus, a higher number of rod-shaped micelles, but with a lower size, will be formed at a higher temperature. This fact leads to a less negative value of ΔS^0_{agg}, providing a higher ΔS^0 value when the T rises.

The increase of ΔH^0_t values (from negative to positive) with an increase in temperature is attributed to the difference in the hydration between the saturated and aromatic hydrocarbon parts of the surfactant [43]. At higher temperatures, the release of water associated with the aromatic ring takes place. This increases the interactions between hydrophobic parts of the closed, making the process endothermic.

From figures 6 and 7, it is observed that ΔH^0_m and ΔS^0_m, as well as ΔH^0_t and ΔS^0_t, are quite sensible to temperature. For the CMC, ΔH^0_m values change from positive to negative as the temperature rises, indicating that the micelle formation process changes from endothermic to exothermic with the temperature. Instead, ΔS^o_m values are always positive, but they become less positive with temperature increases. In figure 9.A both contributions are shown versus temperature for NaDBS, observing that entropic contribution decreases and the enthalpic increases, although in the temperature range examined the entropic part is always higher than the enthalpic one.

Figure 9

In the case of the TMC, the entropic effect dominates again in all temperature range. However, while the entropic contribution increases, the enthalpic one diminishes with the temperature (Figure 9.C).

Enthalpic and entropic contributions to free energy changes have also been analyzed for C_{12}BBr (Figure 9.B and 9.D), using the data reported in reference 10. The results obtained have similar tendencies to those obtained by us (see Figure 9). For the CMC, the process is dominated by the entropic contribution, although this factor decreases and the enthalpy increases with the temperature(Figure 9.B). In the case of the second micellar transition ΔH^0_t diminishes and ΔS^0_t raises with the temperature increase (Figure 9.D). However, in this case a major contribution of enthalpic effect versus entropic was observed below 298 K, but the entropic effect dominates for higher temperatures.

According to this, for both the first and the second critical concentrations, entropy and enthalpy terms are found to compensate each other. When the entropic effect contributes less to the free energy, the enthalpic effect becomes more effective,

and vice-versa. The entropy-enthalpy compensation plot for the first CMC is found to be linear (Figure 10.A), as it has been frequently reported for many surfactants [18, 19, 22-25]. However, we have also observed a linear behavior for the TMC for NaDBS surfactant (Figure 10.B), demonstrating that both processes can be described as follows:

$$\Delta H_m^o = \Delta H_m^* + T_c \Delta S_m^o \quad (15)$$

$$\Delta H_t^o = \Delta H_t^* + T_c^t \Delta S_t^o \quad (16)$$

where, T_c, T^t_c, ΔH^*_m and ΔH^*_t are the temperature compensation of the CMC and TMC and the ΔH^0_m for CMC and TMC when $\Delta S^0_m = 0$, respectively.

Figure 10

The slopes of these plots, T_c and T^t_c, are named constant compensation temperatures and are considered as a characteristic of solute-solvent interactions, that is, of the "desolvation part". There is controversy over the use of these temperature and different authors consider it seems to have no significant physical meaning [23, 25]. For NaDBS, the slopes of the plots in Figure 10 produced T_c= 296 K and T^t_c = 310 K.. These values lie within the suggested literature range 250-315 K [24].

A decrease in ΔH^*_m values with an increase in the alkyl chain length was reported previously [19,22] and it was attributed to a decrease in the stability of the structure of the micelles. From figure 10, for NaDBS ΔH^*_m was -32,73 kJ mol^{-1} and ΔH^*_t -24,94 kJ mol^{-1}. This result may indicate higher hydrophobic interactions in the spherical micelle than in the non spherical one and from this a higher stable structure is expected when the spherical micelle is formed. Furthermore, the compensate plot obtained for C_{12}BBr, using the data reported in reference [8], produces ΔH^*_m equal to -36,52 kJ mol^{-1} and ΔH^*_t equal to -29,61 kJ mol^{-1}. Once again, a higher value resulted for spherical micelles than for non spherical ones, indicating that for this surfactant a major stability is deduced as well for spherical micelles. This idea is in agreement with Alauddin et al. [40], which reported that spherical NaDBS micelles have to be more compact than rod-shaped micelles.

Furthermore, a more negative value of ΔG^0 indicates an increase in the hydrophobic effect [40]. Hence, and knowing that for NaDBS ΔG^0_m is more negative than ΔG^0_t for a same temperature value (Figure 5), hydrophobic forces should be more important in spherical micelles better than non-spherical ones.

5. Conclusions

Sodium dodecylbenzenesulfonate unimer-to-micelle (CMC) and micelle sphere-to-rod (TMC) transitions have been seen by electrical conductivity and surface tension. From electrical conductivity data the thermodynamics of these two transitions has been assessed. ΔH^0 and ΔS^0 decrease with temperature for the CMC of surfactants has been usually interpreted as due to two factors: destruction of the orderly arrangement of water molecules around the hydrophobic chains, and the ordering of the randomly oriented amphiphile molecules from the solvated form into a micelle structure[18, 19, 22, 23]. However, in this work we have shown that ΔH^0 and ΔS^0 increase with the temperature for NaDBS and C_{12}BBr when non-spherical micelles are formed, which cannot be explained by these factors. Also, ΔH^0 and ΔS^0 increase with the temperature has been reported previously for the first CMC for different surfactants[38,43]. These "abnormal" behaviors cannot be explained by the previous factors and, hence, the explanation of ΔH^0 and ΔS^0 variation with the temperature has to be more complicated. Thus, the explanation of ΔH^0 and ΔS^0 variation with the temperature has to include other factors such as ionization of surfactant molecules, thermal solubility of the surfactant monomers, solvation of hydrophilic part of the surfactant molecules, counterionic solvation, coulombic repulsion of the hydrophilic heads, etc. Accordingly, in specific conditions some factors will predominate over the rest which may be neglected.

For the NaDBS and C_{12}BBr surfactants in aqueous solution, at low surfactant concentrations when spherical micelles are formed, ΔH^o and ΔS^0 variation with the temperature will be justified mainly by dehydratation of the hydrophobic chains of the surfactant and the ordering of the randomly oriented amphiphile molecules. However, at higher surfactant concentrations when non-spherical micelles are formed, ΔH^0 and ΔS^0 variation with the temperature values may be explained mainly in terms of an increase in the dehydration of the headgroups and an increase in the thermal solubility of the surfactant monomers.

Finally, it is interesting to note that the compensation ΔH^0- ΔS^0 plot and the ΔG^0 values obtained for the CMC and TMC point to the hydrophobic forces should be more important in spherical micelles better than non-spherical ones, indicating that the former will have a more stable structure than the latter.

Acknowledgements

AJFR would likes to thank the financial support from the Seneca Foundation-Agency of Science and Technology in the Region of Murcia (11955/PI/09) in the framework of the II PCTRM 2007-2010 and the Spanish government (MAT2010-21267-C02-02)

References

1. Tadros T F Applied Surfactants: Principles and Applications, Wiley-VCH, Weinheim, 2005
2. Myers D. Surfaces, Interfaces and Colloids: Principles and Applications, second ed., Wiley-VCH, New York, 1999
3. K. Holmberg, B. Jönsson, B. Kronberg, B. Lindman, Surfactants and Polymers in Aqueous Solution, 2nd edn. Wiley, Chichester, U.K., 2003
4. Treiner C, Makayssi A, Langmuir 8 (1992) 794-800. DOI: 10.1021/la00039a012
5. González-Pérez A, Czapkiewicz J, Prieto G, Rodríguez JR, Colloid Polym Sci 281 (2003) 1191-1195. DOI : 10.1007/s00396-003-0905-2
6. Segota S, Heimer S, Tezak D. Colloids Surf A 274 (2006) 91-99. DOI : 10.1016/j.colsurfa.2005.08.051
7. Rodríguez JR, González-Pérez A, Del Castillo JL, Czapkiewicz J. J. Colloid Interface Sci 250 (2002)438-443. DOI : 10.1006/jcis.2002.8362
8. González-Pérez A, Czapkiewicz J, Ruso JM, Rodríguez JR. Colloid Polym Sci 282 (2004) 1169-1173. DOI : 10.1007/s00396-004-1053-z
9. González-Pérez A, Ruso JM, Prieto G, Sarmiento F. Langmuir 20 (2004) 2512-2514. DOI: 10.1021/la035724d
10. González-Pérez A, Ruso JM. Colloids Surf. A 356 (2010) 84-88. DOI : 10.1016/j.colsurfa.2009.12.034
11. Gao J, Ge W, Li J. Science in China Ser. B Chem. 48 (2005) 470-475. DOI: 10.1360/042004-71
12. Lu X, Jiang Y, Cui X, Mao S, Liu M, Du Y. Acta Phys-Chim Sin 25 (2009) 1357-1361
13. Porte C, Poggi Y. Phys Rev Lett 41 (1978) 1481-1483. DOI: 10.1103/PhysRevLett.41.1481
14. Caron G, Perron G, Lindheimer M, Desnoyers JE. J Colloid Interface Sci 106 (1985) 324-333. DOI: 10.1016/S0021-9797(85)80006-0
15. Paisal R, Martinez R, Padilla J, Fernandez Romero AJ. Electrochim Acta 56 (2011) 6345-6351. DOI:10.1016/j.electacta.2011.05.024
16. Cheng DCH, Gulari E. J Colloid Interface Sci 90 (1982) 410-423. DOI: 10.1016/0021-9797(82)90308-3
17. Gonzalez Y, Nakanishi H, Stjerndahl M, Kaler EW. J Phys Chem B 109 (2005) 11675-11682. DOI : 10.1021/jp050111q
18. Di Michele A, Brinchi L, Di Profio P, Germani R, Savelli G, Onori G. J Colloid Interface Sci 358 (2011) 160-166. DOI : 10.1016/j.jcis.2010.12.028
19. González-Pérez A, Del Castillo JL, Czapkiewicz J, Rodríguez JR. Colloids Surf. A 232 (2004) 183-189. DOI : 10.1016/j.colsurfa.2003.10.018
20. D.F. Evans, H. Wennerström, The Colloidal Domain: Where Physics, Chemistry, Biology, and Technology Meet, 2nd edn.Wiley-VCH, New York, 1999
21. A. Chatterjee, S.P.Moulik, S.K. Sanyal, B.K.Mishra, P.M. Puri, J.Phys. Chem. B 105 (2001) 12823. DOI: 10.1021/jp0123029
22. Chen L, Lin S, Huang C. J Phys Chem B 102 (1998) 4350-4356. DOI: 10.1021/jp9804345
23. Sugihara G, Hisatomi M. J Colloid Interface Sci 219 (1999) 31-36. DOI: 10.1006/jcis.1999.6378
24. Lumry R, Rajender S. Biopolymers 9 (1970) 1125-1227. DOI: 10.1002/bip.1970.360091002

25. Liu G, Gu D, Liu H, Ding W, Li Z. J Colloid Interface Sci 358 (2011) 521-526. DOI: 10.1016/j.jcis.2011.03.064
26. NB Vargaftik, BN Volkov, LD Voljak. J. Phys. Chem. Ref. Data 12 (1983) 817-820
27. Van Os NM, Daane GJ, Bolsman TA. J Colloid Interface Sci 123 (1988) 267-274 DOI: 10.1016/0021-9797(88)90243-3
28. R.F.P. Pereira, A.J.M. Valente, H.D. Burrows, M.L. Ramos, A.C.F. Ribeiro, V.M.M. Lobo. Acta Chim. Slov. 56 (2009) 45-52
29. P. Carpena, J. Aguiar, P. Bernaola-Galván, C.C Ruiz, Langmuir 18 (2002) 6054-6058. DOI: 10.1021/la025770y
30. A.C.F. Ribeiro, V.M.M. lobo, A.J.M. Valente, E.F.G. Azevedo, M.G. Miguel, H.D. Burrows. Colloid Polym. Sci. 283 (2004) 277-283. DOI: 10.1007/s00396-004-1136-x
31. D. Zanette, A.A. Ruzza, S.J. Froehner, E. Minatti. Colloid Surf A. 108 (1996) 91-100. DOI: 10.1016/0927-7757(95)03355-6
32. S.M.C. Silva, F.E. Antunes, J.J.S. Sousa, A.J.M. Valente, A.A.C.C. Pais. Carbohydrate Polym. 86 (2011) 35-44. DOI: 10.1016/j.carbpol.2011.03.053
33. S.Y. Lin, Y.Y. Lin, E.M. Chen, C.T. Hsu, C.C. Kwan. Langmuir 15 (1999) 4370-4376. DOI: 10.1021/la981149f
34. RG Alargova, KD Danov, JT Petkov, PA Kralchevsky, G. Broze, A. Mehreteab. Langmuir 13 (1997) 5544-5551. DOI: 10.1021/la970399d
35. M Wang, S Kong, S Liu, C. Li, M Wang, Y. Tan. Colloids Surf A: Physicochem Eng. Asp. 441 (2014) 25-33. DOI : 10.1016/j.colsurfa.2013.08.066
36. J. D. Rouse, D. A. Sabatini, J. H. Harwell. Environ. Sci. Technol. 27 (1993) 2072–2078. DOI: 10.1021/es00047a012
37. Muller N. Langmuir 9 (1993) 96-100. DOI: 10.1021/la00025a022
38. Islam MN, Kato T. J Phys Chem B 107 (2003) 965-971. DOI : 10.1021/jp021212g
39. A Krofic, B. Sarac, M. Bester-Rogac. J. Chem Thermodynamics 43 (2011) 1557-1607. DOI:10.1016/j.jct.2011.05.015
40. Alauddin M, Rao NP, Verrall RE. J Phys Chem 92 (1988) 1301-1307. DOI: 10.1021/j100316a057
41. Bhat MA, Dar AA, Amin A, Rashid PI, Rather GM. J Chem Thermodynamics 39 (2007)1500-1507. DOI: 10.1016/j.jct.2007.02.011
42. Heerklotz H, Tsamaloukas A, Kita-Tokarczyk K, Strunz P, Gutberlet T. J Am Chem Soc 126 (2004)16545-16552. DOI: 10.1021/ja045525w
43. Kabir-ud-Din, Rub MA, Naqvi AZ. J Colloid Interface Sci 354 (2011) 700-708. DOI : 10.1016/j.jcis.2010.11.005

Figure Captions

Figure 1. Specific conductivity vs. NaDBS concentration at different temperatures.

Figure 2. Mole fractions of CMC;●, and TMC;■, as a function of temperature of NaDBS, as determined by electrical conductivity measurements.

Figure 3. Degree of ionizations β and β_t as a function of temperature as computed from electrical conductivity measurements.

Figure 4. Normalised surface tension as a function of concentration of NaDBS at different temperatures. 298 K;□, 303 K;o, 308 K;Δ, and 313 K;◊. Solid lines represent to the best fit of a straight line equation to the experimental data.

Figure 5. ΔG^0_m;●, and ΔG^0_t;■, versus temperature of NaDBS.

Figure 6. Enthalpy changes versus temperature. A) ΔH^0_m;●, and ΔH^0_t;■,obtained using equations (3,4) and ΔH^0_m;○, and ΔH^0_t;□, obtained applying the Muller's treatment for NaDBS. B) ΔH^0_m;●, and ΔH^0_t;■, obtained using equations (3,4) for C_{12}BBr.

Figure 7. Entropy changes versus temperature. A) ΔS^0_m;●, and ΔS^0_t;■, of NaDBS obtained using equations (5,6) and ΔS^0_m;○, and ΔS^0_t;□, obtained applying the Muller's treatment. B) ΔS^0_m;●, and ΔS^0_t;■, of C_{12}BBr obtained using equations (5,6).

Figure 8. $\ln(\chi_{cmc}/\chi^*_{cmc})$ vs. $(1-T^*/T+\ln T^*/T)\cdot 1/(2-\beta)R$ for the CMC;●, and $\ln(\chi_{tmc}/\chi^*_{tmc})$ vs. $(1-T_t^*/T+\ln T_t^*/T)\cdot 1/(2-\beta_t)R$ for TMC;■, of NaDBS.

Figure 9. Enthalpic;●, and Entropic;■, contribution to ΔG^0_m and ΔG^0_t of NaDBS at various temperatures (A, C). Enthalpic;●, and Entropic;■, contribution to ΔG^0_m and ΔG^0_t of C_{12}BBr (B, D) at various temperatures.

Figure 10. Enthalpy-entropy compensation plots of the CMC (A) and TMC (B) for NaDBS;●, and C_{12}BBr;■,.

Figure 1

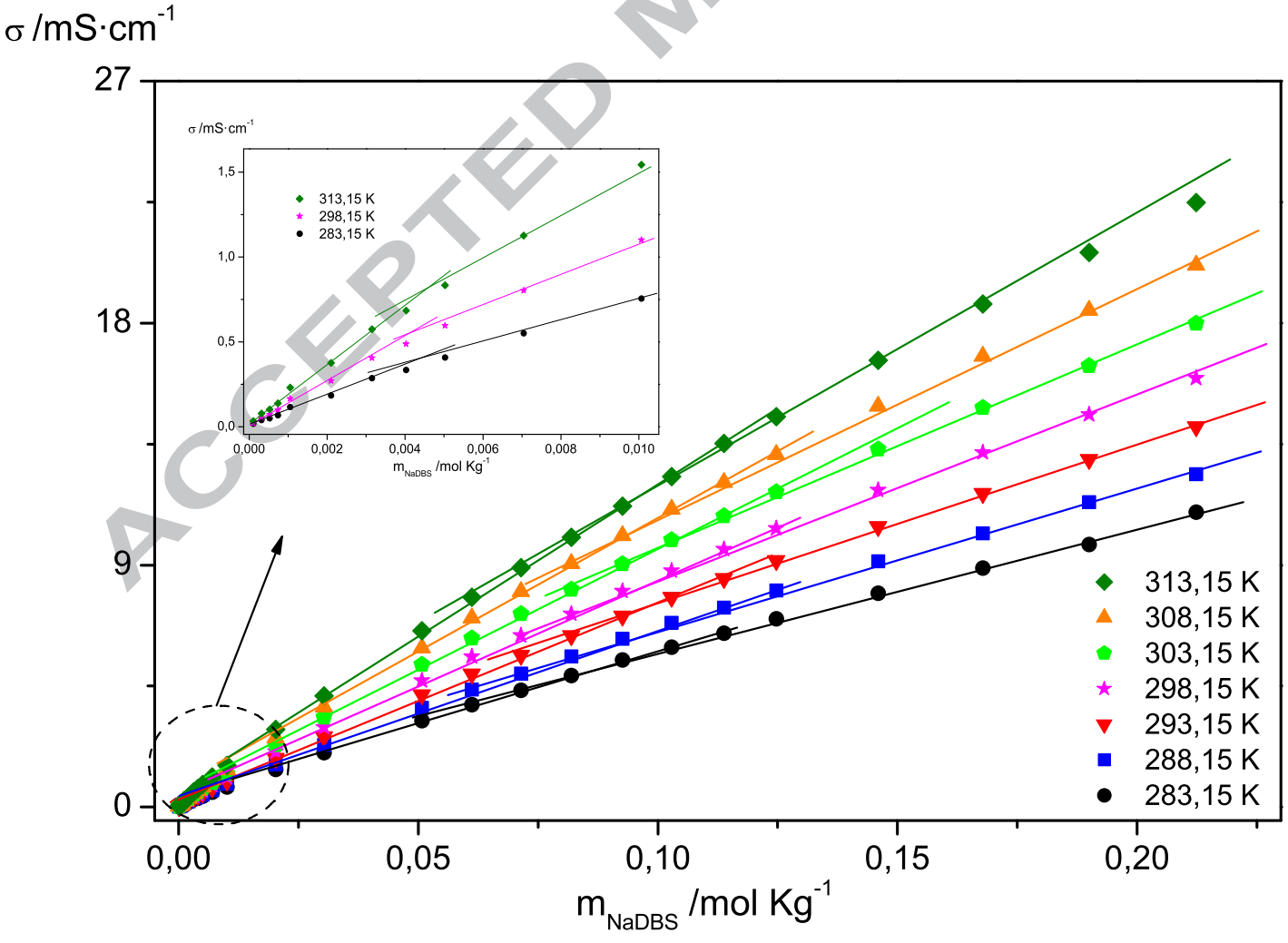

Figure 2

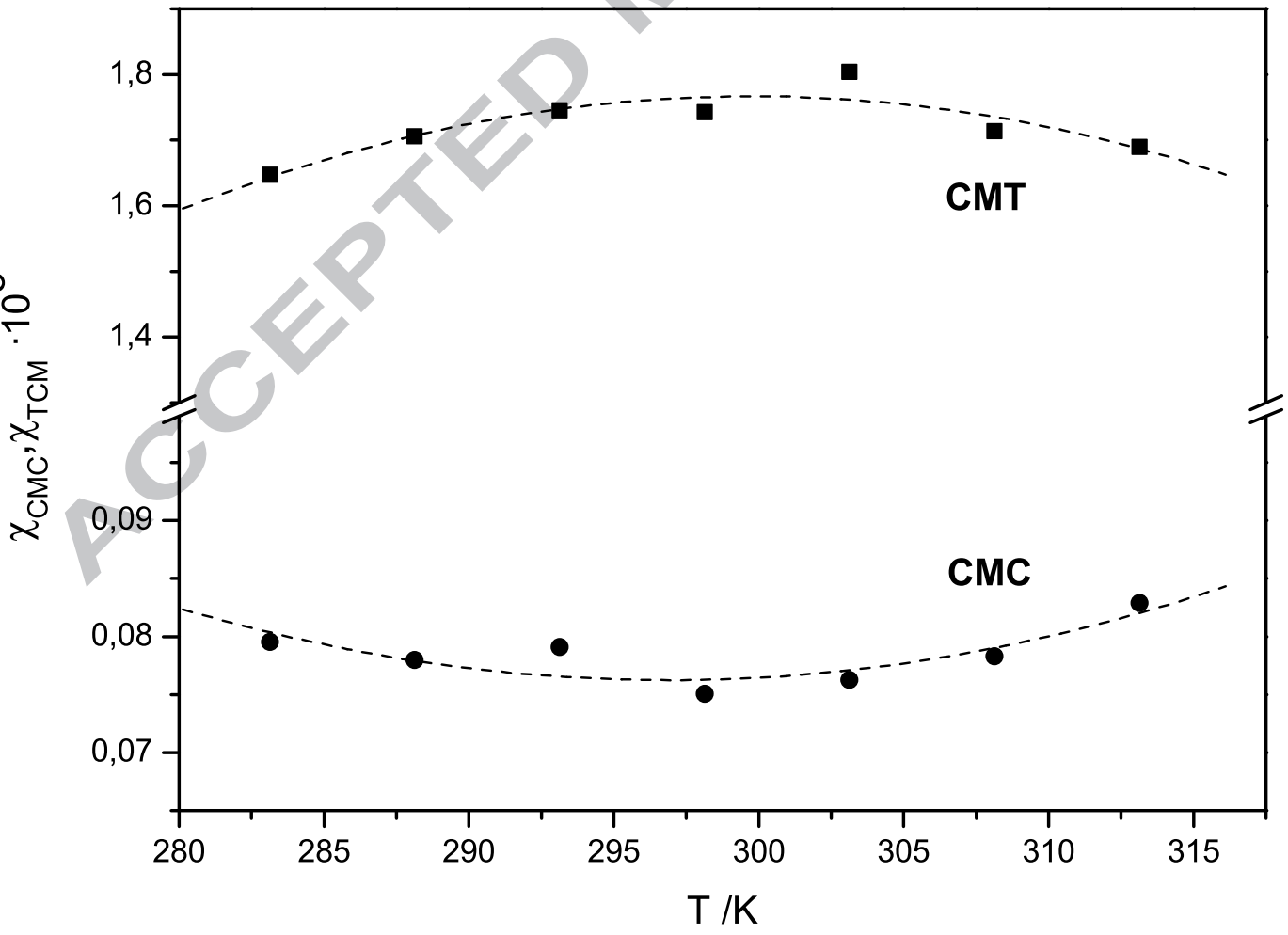

Figure 3

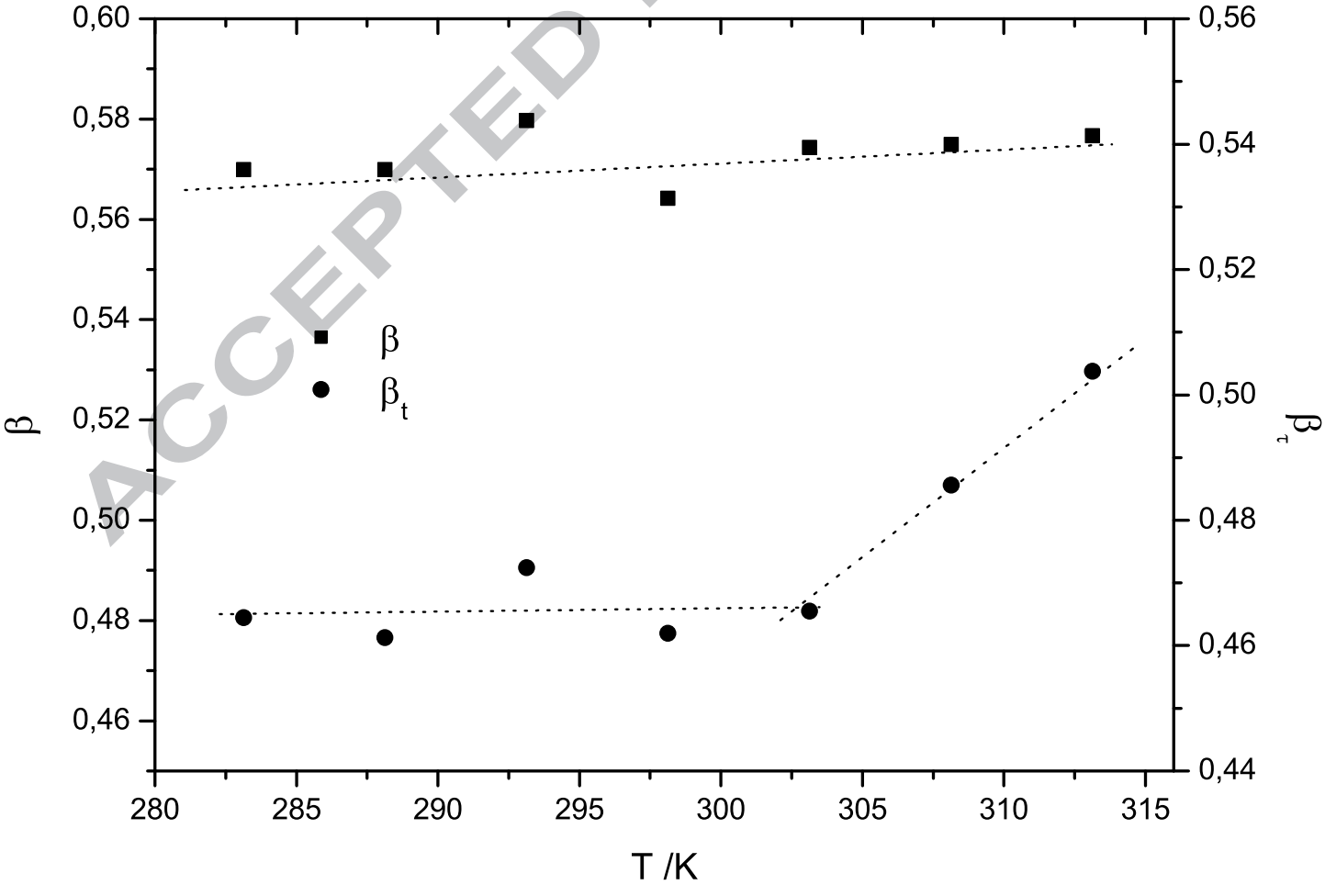

Figure 4

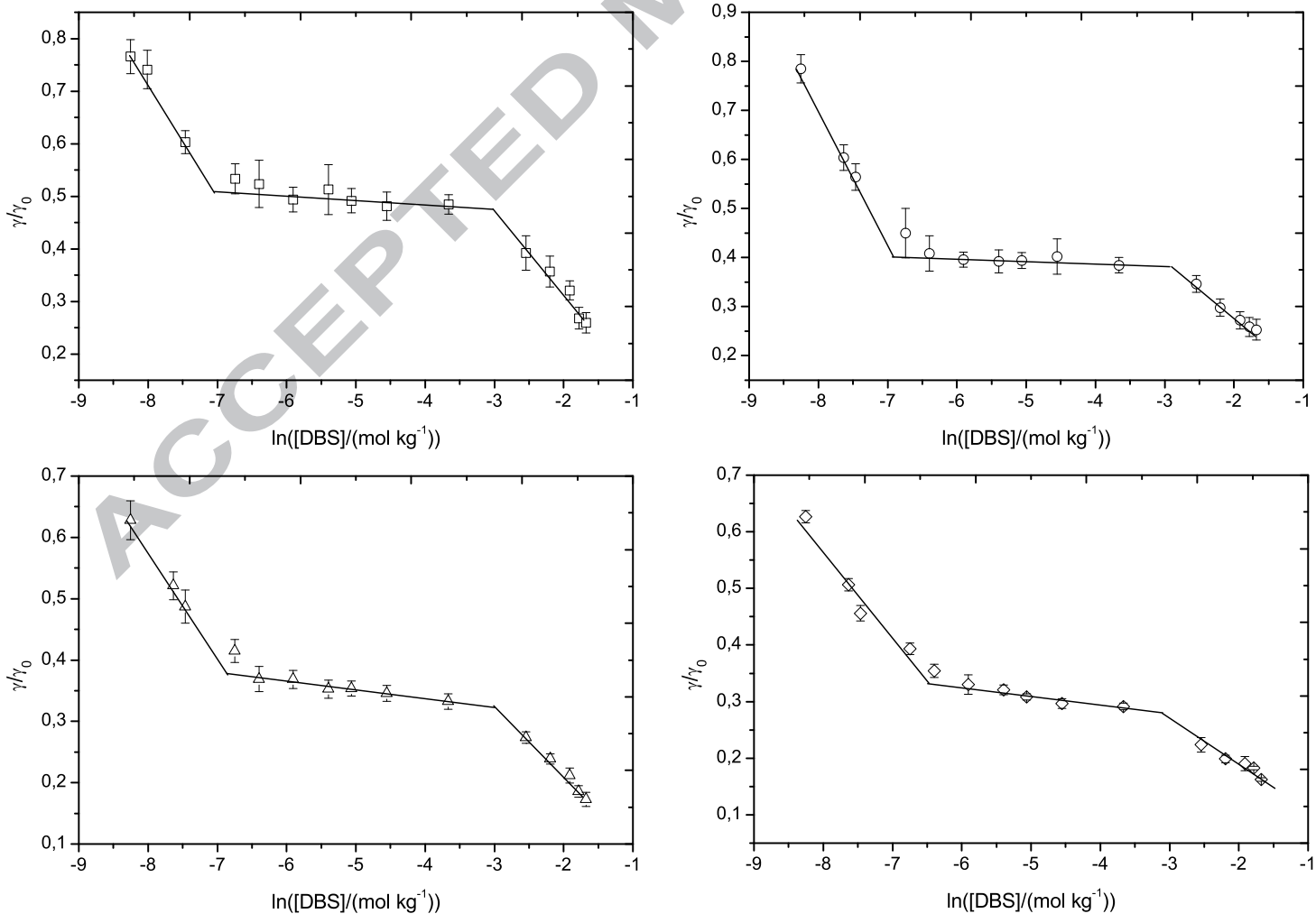

Figure 5

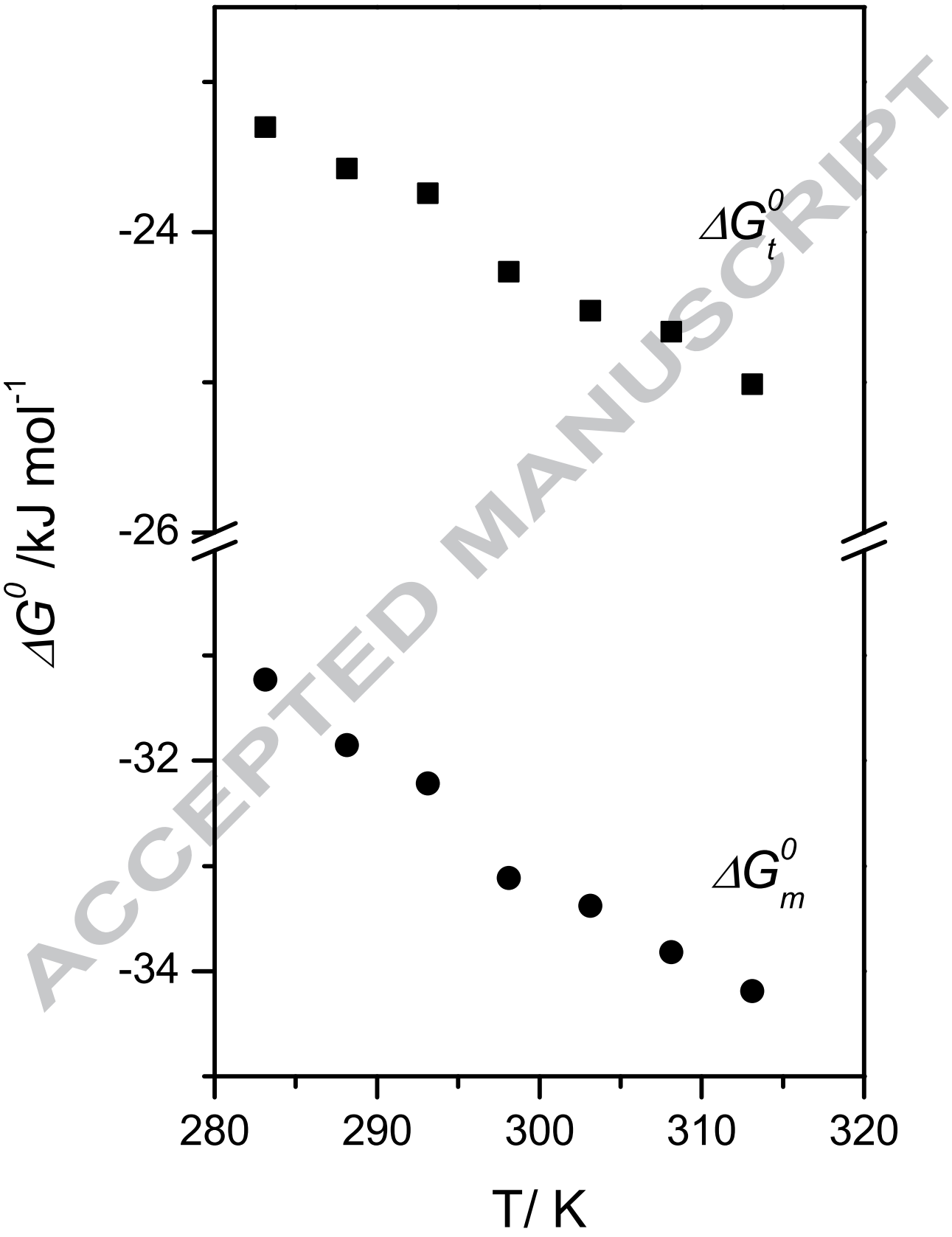

Figure 6

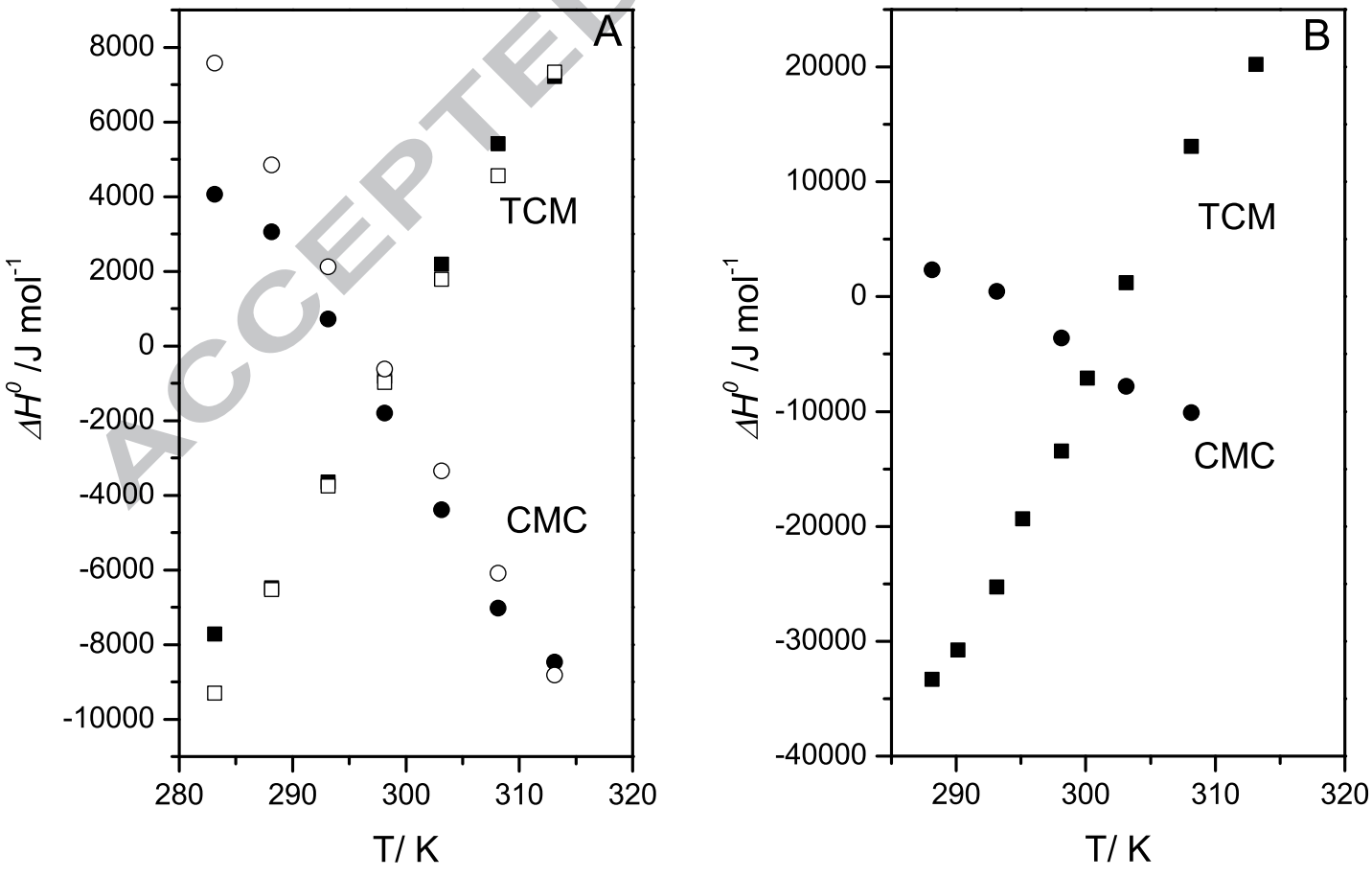

Figure 7

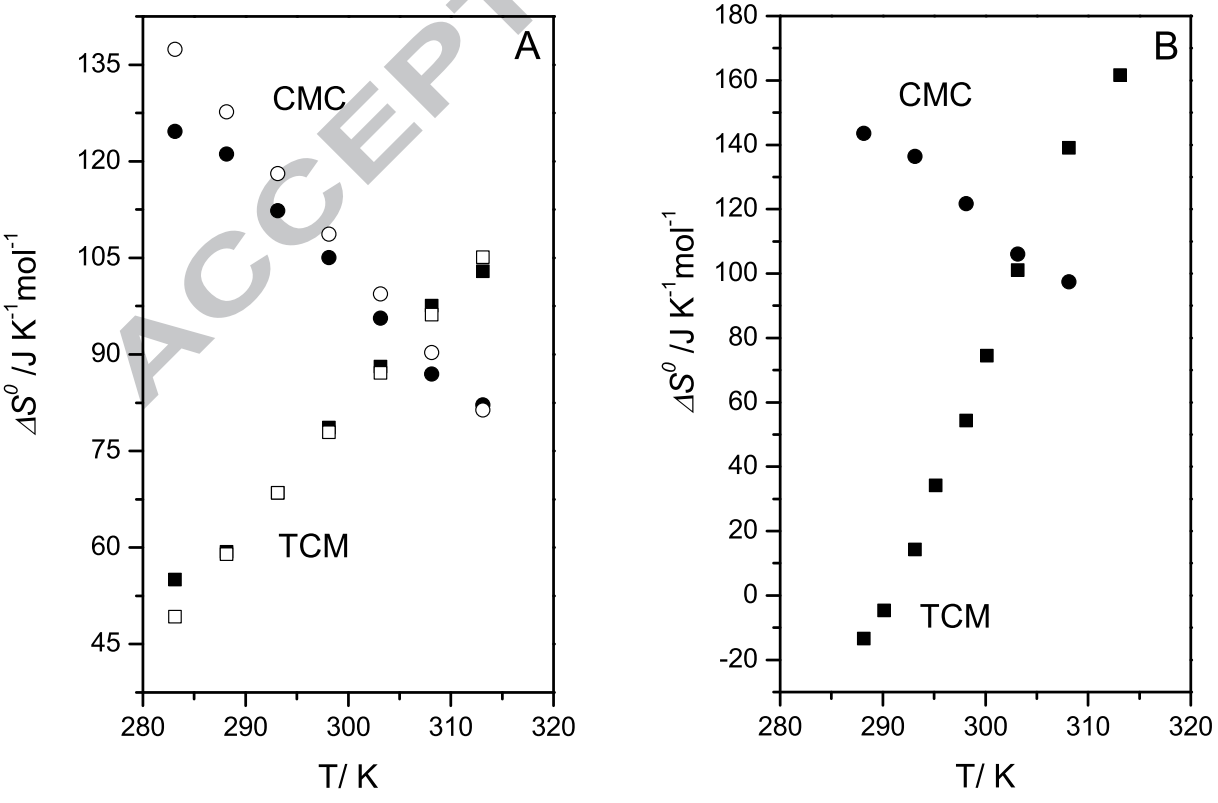

Figure 8

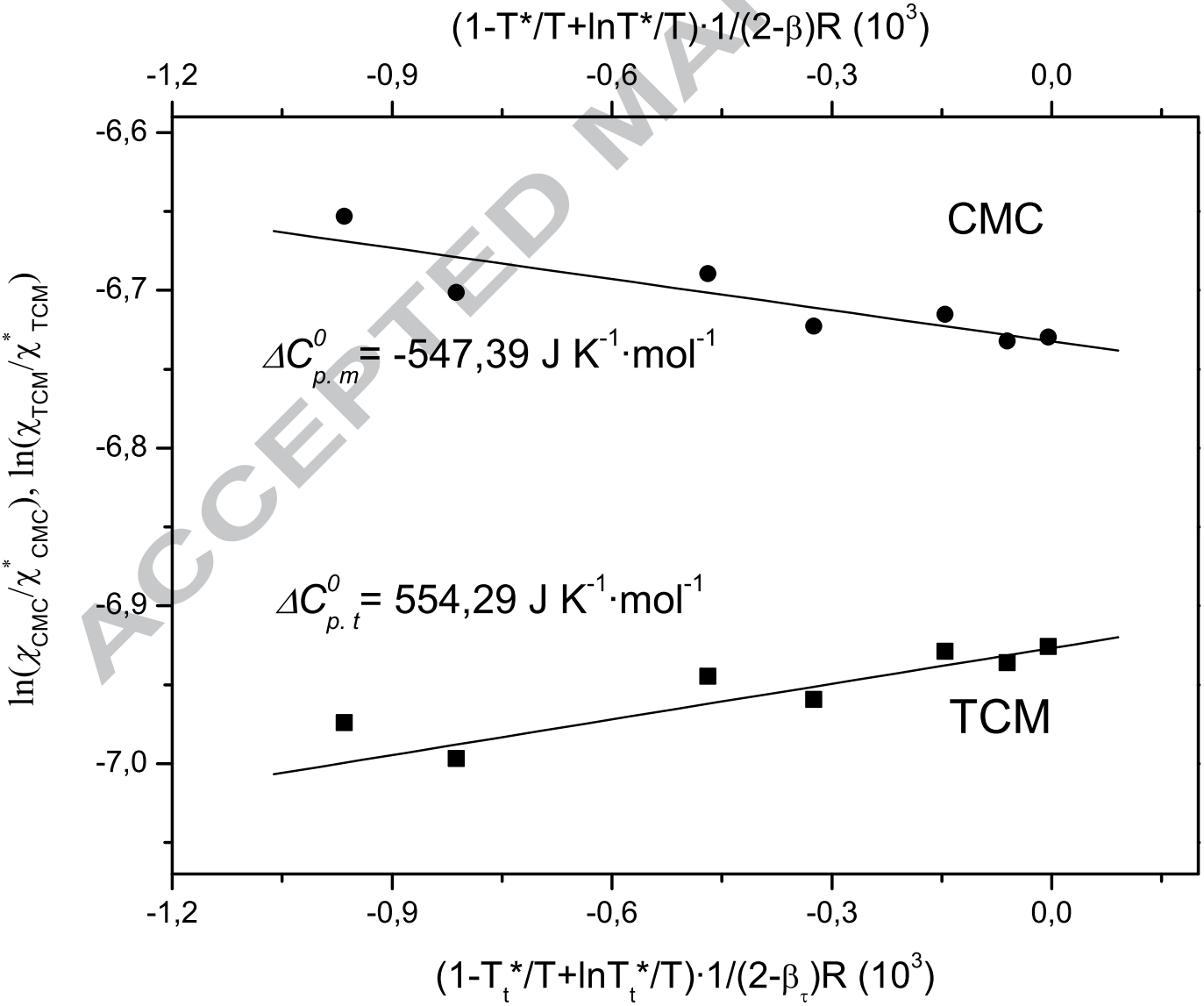

Figure 9

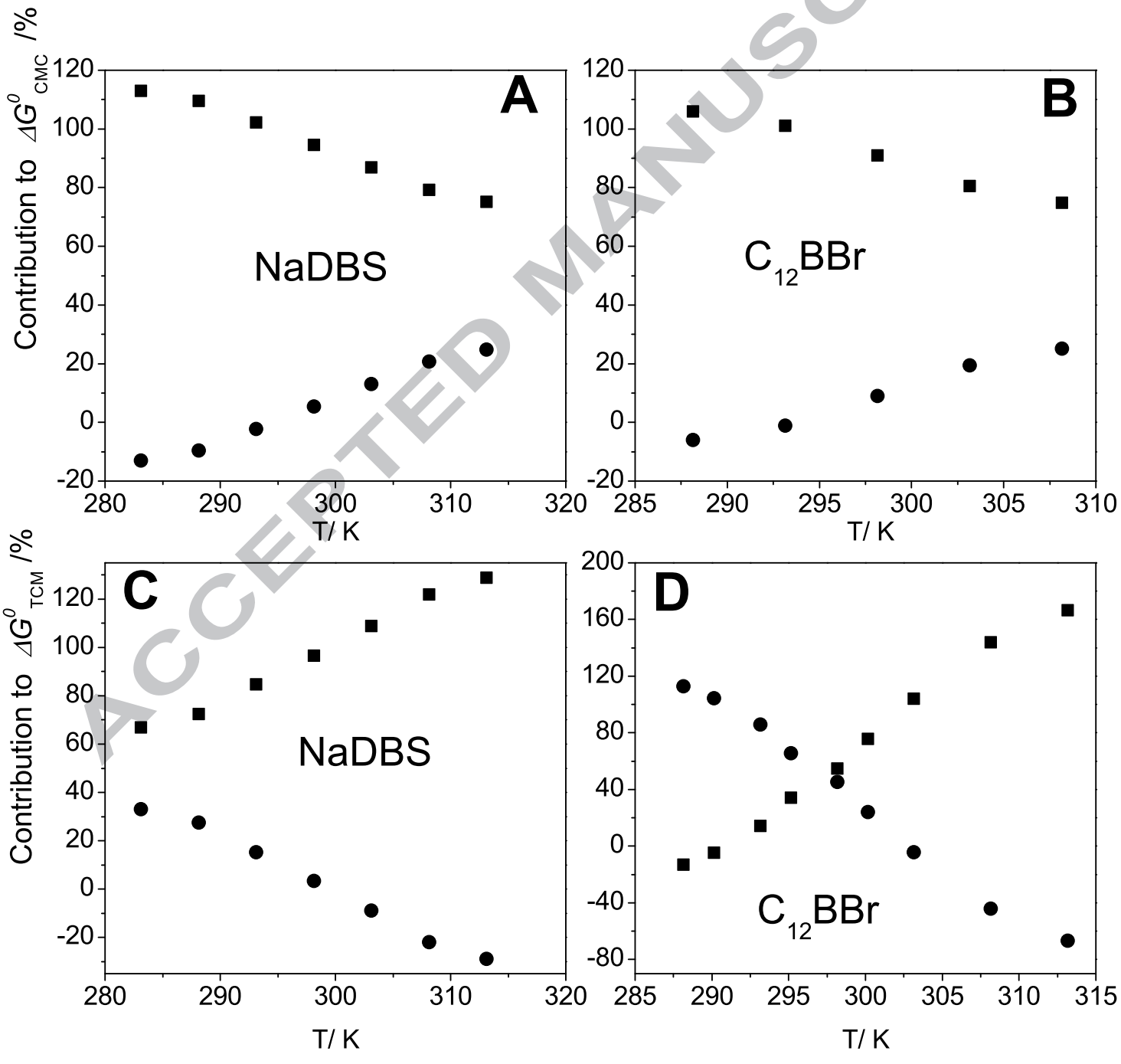

Figure 10

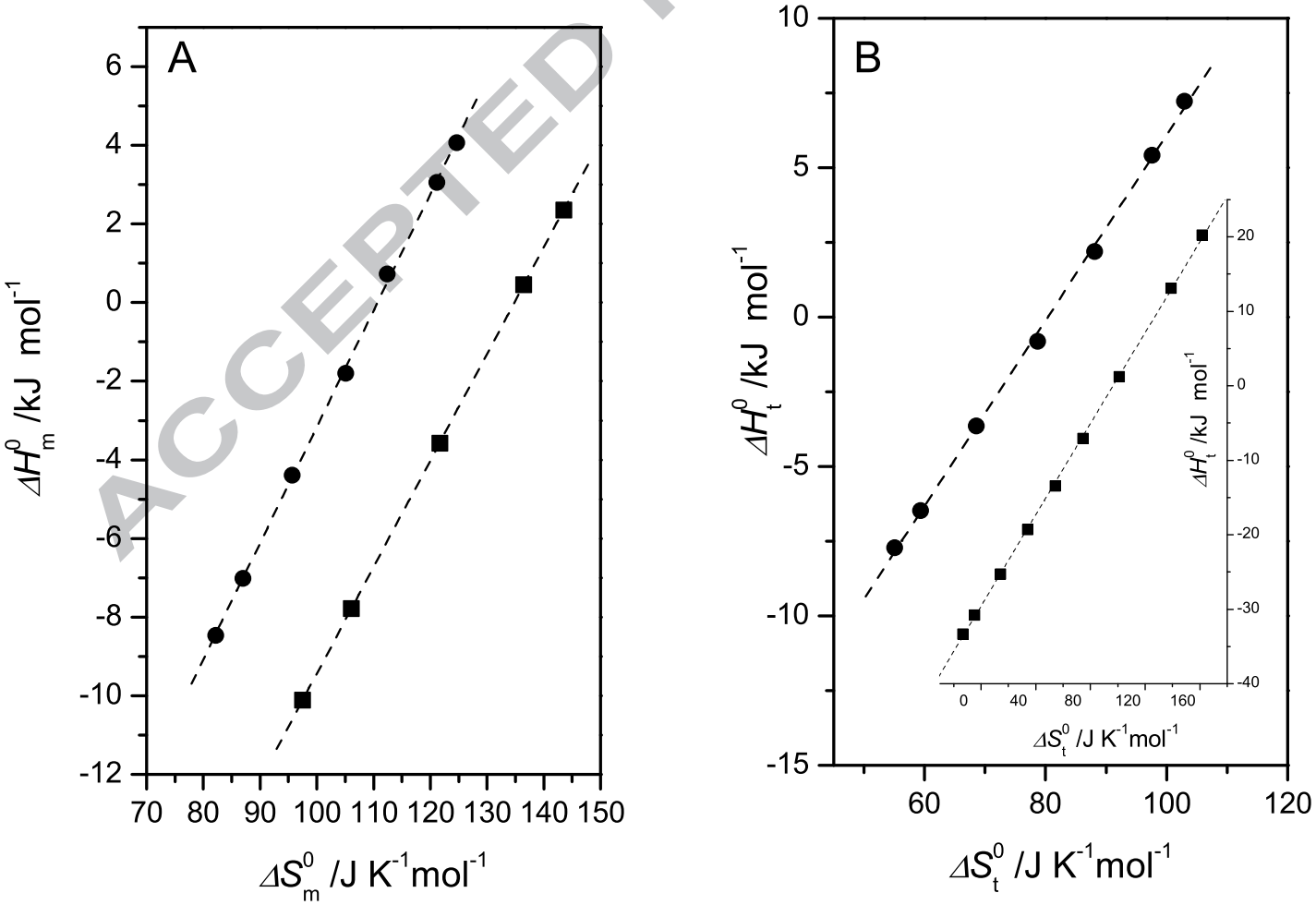

Table 1. Variation of the critical and transition micellar concentrations of NaDBS values (and the standard deviations of the mean) with the temperature as measured by surface tension measurements, at P=1.01×10^5 Pa.

T / K	298.15	303.15	308.15	313.15
CMC /mmol Kg^{-1}	0.91 (± 0.04)	1.00 (± 0.06)	1.03 (± 0.07)	1.55 (± 0.03)
TMC /mmol Kg^{-1}	50.3 (± 2.0)	53.4 (± 2.1)	50.3 (± 3.0)	45.9 (± 4.1)

u(T)=0.02 K; u(P)=1×10^3 Pa.

Graphical abstract

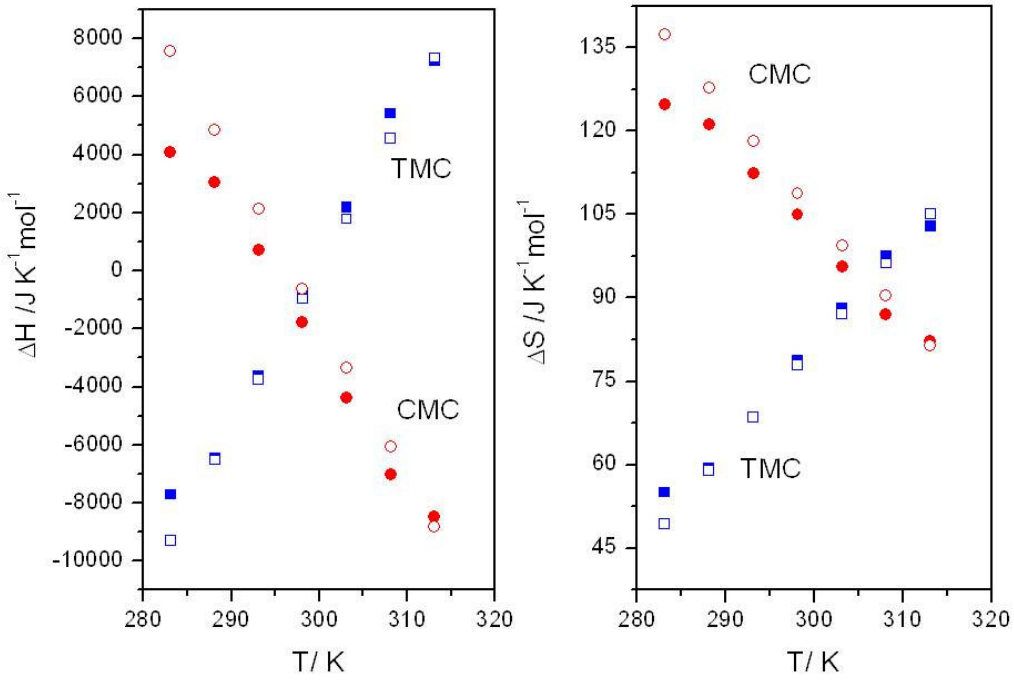

Highlights

Unimer-micelle and sphere-to-rod micellar transitions were observed to sodium dodecylbenzenesulfonate in aqueous solutions

Two micellar transitions were seen by electrical conductivity and surface tension

An anomalous ΔS^0 and ΔH^0 increase with T was found for the second critical transition

More stable aggregates are evidenced for spherical micelles than for the other shapes